Polyisobutylene-Toughened Poly(methyl methacrylate). 2. Small-Angle X-ray Scattering Analysis of Microdomain Morphology of a Series of PMMA-*l*-PIB Networks

Thein Kyu,† Joseph P. Kennedy,*,‡ and G. Caywood Richard‡

Institute of Polymer Science, The University of Akron, Akron, Ohio 44325-3909, and Institute of Polymer Engineering, The University of Akron, Akron, Ohio 44325-0301

Received April 1, 1992; Revised Manuscript Received October 20, 1992

ABSTRACT: A series of new polyisobutylene (PIB)-toughened poly(methyl methacrylate)s (PMMA) consist of PIB domains covalently bonded to a PMMA matrix. The broad maxima observed in the small-angle X-ray scattering (SAXS) profiles indicate microphase-separated materials containing PIB microdomains dispersed within a PMMA matrix. SAXS was used to determine the effect of PIB molecular weight ($\bar{M}_n$) and weight percent (wt %) on the long period (L, repeat distance of electron density variation) in the materials. L and the maximum intensity of the scattering peak were found to increase with increasing $\bar{M}_n$ and wt % PIB, indicating larger dispersed PIB microdomains. The good agreement between measured and calculated values of the mean square electron density fluctuation, $\langle\eta^2\rangle$ normalized with respect to the 18K5 sample, indicates that the overall compositions of the PMMA-*l*-PIB networks are close to targeted values.

Introduction

The goal of this research was to study the effect of polyisobutylene (PIB) $\bar{M}_n$ and wt % on the microstructure of PIB-modified poly(methyl methacrylate)s (PMMA)s. Living carbocationic polymerization of isobutylene[1,2] permits precise control of PIB $\bar{M}_n$, which in turn influences mechanical properties. Three different $\bar{M}_n$ methacrylate telechelic PIBs (6500, 18 000, and 37 000 g/mol) were prepared. The functionalizations were effected by an established reaction sequence[3-5] to prepare methacrylate-terminated tritelechelic PIB macromomoners [PIB-$(MA)_3$]. The copolymerization of PIB-$(MA)_3$ with methyl methacrylate (MMA) to form new PMMA-*l*-PIB semisimultaneous interpenetrating networks (semi-SINs) along with their characterization was reported in paper 1 of this series.[6] Because of the simultaneous formation of the network and PMMA homopolymer portions, PMMA-*l*-PIBs are semi-SINs.[7] Since the polymerizations of the two comonomers [PIB-$(MA)_3$ and MMA] are not mutually exclusive, two-component PMMA-*l*-PIB networks, together with PMMA homopolymer, are formed. Therefore, these materials represent a new type of semi-SIN.

For the study of the effect of wt % PIB on L, a series of semi-SINs composed of 5, 10, 20, and 30 wt % PIB-$(MA)_3$ of $\bar{M}_n$ = 18 000 g/mol and PMMA were analyzed by SAXS. To determine the effect of $\bar{M}_n$ on L, samples containing 20 wt % PIB of three PIB-$(MA)_3$s (i.e., $\bar{M}_n$ = 6500, 18 000, and 37 000 g/mol) were employed.

Experimental Procedures

The synthesis and characterization of PMMA-*l*-PIB semi-SINs have been described.[6] SAXS experiments were conducted at Oak Ridge National Laboratories using a 10 M SAXS system coupled with a two-dimensional position-sensitive detector for rapid analysis of multiphase samples. A 12-kW Rigaku X-ray generator equipped with a copper target was operated at 80 mA and 40 kV. The sample to detector distance was 5.12 m to cover the scattering range 0.08–1.2 nm^{-1}. For the calculation of $\langle\eta^2\rangle$, a constant electron density within each of the two phases (PIB and PMMA) was assumed, with phases separated by sharp boundaries. Q, the scattering invariant (for calculation of measured values of $\langle\eta^2\rangle$, was determined by computer integration of the area under the Lorentz corrected scattering curve.[8] The materials studied are listed in Table I, with identification codes according to PIB $\bar{M}_n$ and wt % in the sample.

Results and Discussion

After having synthesized new PMMA-*l*-PIB semi-SINs, it was of interest to determine the effect of PIB $\bar{M}_n$ and wt % on L and to correlate this quantity with mechanical properties. The tensile properties of these materials have been thoroughly investigated.[6]

Figure 1 illustrates the two-dimensional scattering pattern for sample 6K20. The lighter areas indicate maximum scattering intensity. The scattering ring suggests microphase separation and random orientation. To show the effect of $\bar{M}_n$ on the microstructure, the Lorentz corrected scattering profiles of samples 6K20, 18K20, and 37K20 are shown in Figure 2. The Lorentz corrected scattering profiles of the 18K series containing various amounts of PIB are illustrated in Figure 3. The scattering profiles exhibit a scattering peak or, in the case of 18K5 and 18K10, a broad shoulder characteristic of a periodic variation of electron density. The average repeat distance of this variation can be estimated from the peak position by Bragg's law[8]

$$\lambda = 2L \sin\theta \tag{1}$$

where L is the repeat distance of the electron density variation, 2θ the scattering angle, and λ the wavelength of the X-ray radiation (1.54 Å of the Cu Kα line). The scattering vector (q, wavenumber) is determined by[8]

$$q = [4\pi/\lambda] \sin\theta \tag{2}$$

The quantity q_{max} is determined from the maximum of the Lorentz corrected plot of $q^2I(q)$ vs q and is used to determine the repeat distance by[8]

$$L = (2\pi)/q_{max} \tag{3}$$

The L values obtained in this manner qualitatively indicate the scale of the electron density variation.

Table II provides L values determined in this manner. Figures 4 and 5 illustrate the effect of PIB $\bar{M}_n$ and wt % on L. The scattering profiles indicate a strong dependence of L on $\bar{M}_n$. Increasing PIB $\bar{M}_n$ results in a decrease in q_{max} and therefore an increase in L. However, the increase in L with increasing PIB wt % is subtle relative to that

* Author to whom correspondence should be addressed.
† Institute of Polymer Science.
‡ Institute of Polymer Engineering.

0024-9297/93/2226-0572$04.00/0

Table I
Sample Identification Codes

sample	PIB $\bar{M}_n$ (g/mol)	PIB wt %
18K5	18 000	5
18K10	18 000	10
18K20	18 000	20
18K30	18 000	30
6K20	6 500	20
37K20	37 000	20

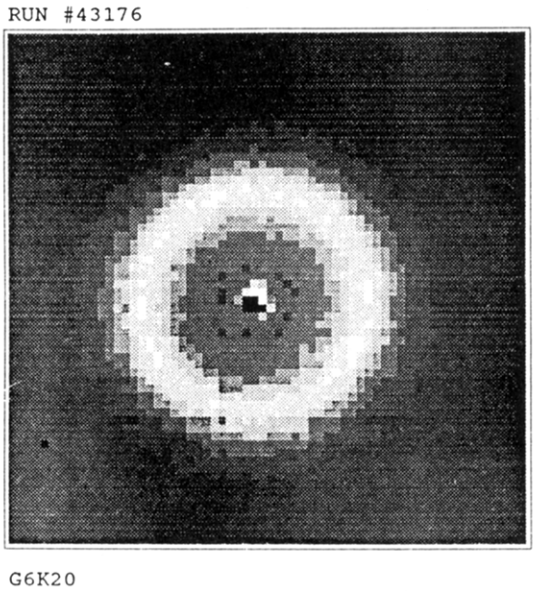

Figure 1. Two-dimensional scattering pattern for 6K20 PMMA-*l*-PIB semi-SIN.

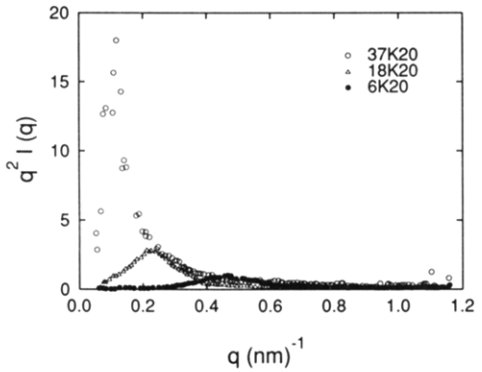

Figure 2. Lorentz corrected scattering profiles of 6K20, 18K20, and 37K20 PMMA-*l*-PIB semi-SINS.

with $\bar{M}_n$. Two models may be invoked to account for the effect of PIB $\bar{M}_n$ and wt % on the observed SAXS peak. One possibility is the core-shell model proposed by MacKnight and co-workers[9] for ionic polymers where ionic spheres (clusters) are surrounded by nonionic chains. In view of the synthesis technique used,[6] the PIB domains may be viewed to consist of an aromatic ring surrounded by aliphatic PIB chains (see Figure 1 in ref 6). The electron density contrast between the aromatic core and PIB shell may give rise to a SAXS peak. These concentric core-shell spheres are dispersed in the continuum of cross-linked PMMA matrix. Depending upon how these PIB domains are distributed in the PMMA matrix, interparticle interferences could occur, leading to an interference SAXS peak. In this model, the electron density contrast between the PIB domain and the PMMA matrix would give rise to the SAXS intensity. The interpretations of L for the core-shell model and for the interparticle interference model are vastly different. In the former, L is the diameter

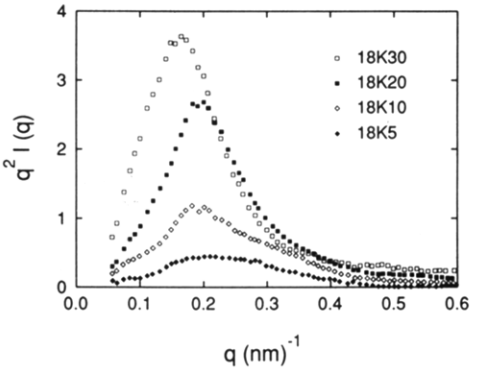

Figure 3. Lorentz corrected SAXS profiles of 18K series of PMMA-*l*-PIB semi-SINs.

Table II
L, $\langle\eta^2\rangle$, and Q As Obtained by SAXS

sample	L (nm)	Q (nm^{-6})	$\langle\eta^2\rangle_{expt}$	$\langle\eta^2\rangle_{calcd}$
18K5	29.92	0.14	1.000	1.000
18K10	34.91	0.29	2.071	1.895
18K20	33.07	0.51	3.643	3.368
18K30	40.54	0.70	5.000	4.421
6K20	15.32			
37K20	62.18			

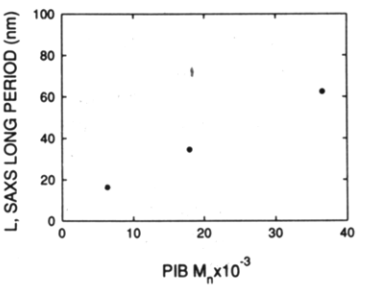

Figure 4. Variation of long period with PIB $\bar{M}_n$ (measured with 20 wt % PIB samples).

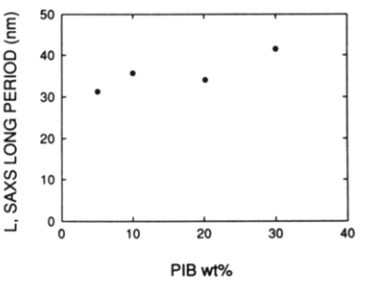

Figure 5. Variation of long period with wt % PIB (measured with 18K series).

of the concentric core-shell, whereas in the latter it represents the interdomain distance.

When PIB $\bar{M}_n$ increases, the diameter of the PIB domains increases, and therefore L would also increase. Correspondingly, the center-to-center mass distance between PIB domains could increase with increasing $\bar{M}_n$. However, the amount of the aromatic center relative to the PIB domains and the PMMA matrix is insignificant, so that the core-shell model alone may be inadequate to account for the large increase in I (integrated scattered intensity).

With increasing PIB content L increases gradually but nonlinearly. A simple "domain insertion model", where the domain population increases with increasing PIB content, would predict a decrease in L. Alternatively, the core-shell model would predict L to remain constant with wt % PIB provided that the $\bar{M}_n$ of PIB remains constant,

which is contradictory to the observations. As pointed out in a preceding paper,[6] the 30 wt % PIB specimen is slightly opaque, suggesting the existence of structures comparable to or larger than the wavelength of light; thus, it is beyond the resolution of SAXS.

Aggregation of PIB domains is a possibility, although no direct evidence was obtained by transmission electron microscopy. A significant drop-off in tensile strength and toughness is noted above 20 wt % PIB, which may be due to increased PIB domain aggregations or, possibly, the onset of a "semicontinuous" PIB phase.[6] Thus, aggregation of PIB domains may follow the interparticle interference model at greater than 20 wt % PIB.

The effect of PIB $\bar{M}_n$ and wt % on the scattered intensity (I integrated intensity) has been examined. As pointed out previously, the volume fraction of the aromatic center of the PIB domains is too small to account for the large increase in the scattered intensity. We therefore adopt the pseudo-two-phase model (neglecting the aromatic core of the PIB domains) in which PIB domains are dispersed in a PMMA matrix.

The 18K series was analyzed in terms of calculated and measured $\langle\eta^2\rangle$ values. The calculated values were determined by[8]

$$\langle\eta^2\rangle = \phi_1\phi_2(\rho_1 - \rho_2)^2 \tag{4}$$

where ϕ_1 and ϕ_2 are the volume fractions of the matrix and PIB, respectively, and ρ_1 and ρ_2 the electron density of PMMA and PIB, respectively. A constant electron density within each of the two phases is assumed, with phases separated by sharp boundaries. Values of $\langle\eta^2\rangle$ were normalized with respect to sample 18K5.

The measured $\langle\eta^2\rangle$ value was then determined by calculating Q, the scattering invariant, from the integration of the area under the Lorentz corrected scattering curves according to[8]

$$Q = \int I(q)q^2 dq \tag{5}$$

where $I(q)$ is the scattering intensity as a function of wavenumber. Once Q is known, $\langle\eta^2\rangle$ can be obtained from[8]

$$Q = 2\pi^2 I_e V\langle\eta^2\rangle \tag{6}$$

where I_e is the scattering from one electron (Thompson scattering) and V the illumination volume. Both experimental and calculated $\langle\eta^2\rangle$ values were normalized with respect to the 18K5 specimen. Results obtained for Q and $\langle\eta^2\rangle_{expt}$ are listed in Table II, along with $\langle\eta^2\rangle_{calcd}$.

The good agreement obtained between the calculated and measured $\langle\eta^2\rangle$ values indicates that the compositions (wt % PIB) of the PMMA-*l*-PIB semi-SINs are very close to targeted values. The overall appearance of the scattering profiles indicates that the products are microphase-separated. The PIB domain size increases primarily with increasing PIB $\bar{M}_n$ and by increasing the PIB content to ≥20 wt %.

Acknowledgment. We thank Drs. J. S. Lin and M. H. Cho for conducting SAXS experiments at Oak Ridge National Laboratories.

References and Notes

(1) Faust, R.; Kennedy, J. P. *J. Polym. Sci., Part A: Polym. Chem.* **1987**, *25*, 1847.
(2) Kaszas, G.; Puskas, J.; Kennedy, J. P. *Makromol. Chem., Macromol. Symp.* **1988**, *13/14*, 473.
(3) Kennedy, J. P.; Chang, V. S. C.; Smith, R. A.; Ivan, B. *Polym. Bull.* **1979**, *1*, 575.
(4) Ivan, B.; Kennedy, J. P.; Chang, V. S. C. *J. Polym. Sci., Part A: Polym. Chem.* **1980**, *18*, 3177.
(5) Kennedy, J. P.; Hiza, M. *J. Polym. Sci., Part A: Polym. Chem.* **1983**, *21*, 1033.
(6) Kennedy, J. P.; Richard, G. C. *Macromolecules* **1993**, preceding paper in this issue.
(7) Sperling, L. H. *Interpenetrating Polymer Networks and Related Materials*; Plenum Press: New York, 1981.
(8) Porod, G. In *Small Angle X-Ray Scattering*; Glatter, O., Kratky, O., Eds.; Academic Press: London, 1982; p 17.
(9) MacKnight, W. J.; Taggart, W. P.; Stein, R. S. *J. Polym. Sci., Part C: Polym. Lett.* **1974**, *45*, 113.